

**Final Report:**  
**Estuarine Hydrodynamic Modeling of Rookery Bay**

**DEP Contract #RM050**  
**Contract received 8/16/06**

**by**

**Robert H. Weisberg**

**and**

**Lianyuan Zheng**

**College of Marine Science**  
**University of South Florida**  
**140 7th Avenue South**  
**St. Petersburg, FL 33701**

**September 10, 2007**

## **1. Introduction**

A project entitled: “Estuarine hydrodynamic modeling of Rookery Bay” was initiated in August 2006 with support from the Florida Department of Environmental Protection. Initially granted for a one-year duration, the goal of the project was to develop a three-dimensional (3D), baroclinic, prognostic estuarine circulation (hydrodynamic) model that could be used to describe and understand the circulation of the Rookery Bay (RB) estuary system and study the relationship between the freshwater inflows (cfs) from the Henderson Creek (HC) and Eagle Creek canals and the salinity patterns within both HC and the larger scale RB estuary complex. While not a part of the original proposal it was decided during the process of model grid generation to also include Naples Bay (NB) in the overall model domain. The reasons for this addition were based on the following: 1) the potential exists for water exchange between NB and RB and 2) there are no 3D, baroclinic, hydrodynamic models available for NB. This decision for expanding the model domain to include NB was facilitated by the availability of high resolution of bathymetry for NB from the South Florida Water Management District (SFWMD) and a NOAA-NOS tide gauge is available for quantifying the model simulation veracity. This final report describes the activities of the University of South Florida investigators, L. Zheng and R.H. Weisberg, in the conduct of the proposed research, presents important findings, and offers suggestions for future work as part of our conclusions.

## **2. Description of the Rookery Bay estuary complex and Henderson Creek**

The RB estuary complex (of which HC is a part of) is located in southwest Florida between the Ten Thousand Islands to the south and NB to the north (Fig. 1). The estuary is landward of Keewaydin Island, the barrier-island that separates the RB estuary complex from the adjacent Gulf of Mexico (GOM). Combined, the surface area of RB and HC is about 1400 acres, and the estuary system includes mangroves, submerged aquatic vegetation, and reef habitats. Water depths within the RB complex range between 0 to 3 m, with mean values of 1 m in RB and 0.75 m in HC.

The exchanges of water and other materials between the RB estuarine complex and the GOM occur through two inlets, one located at northwest end of RB (section I) and the other at Hall Bay (section II) (Fig. 2). The water movement within the estuarine complex is dominated by tides. Previous observations (Lee and Yokel, 1973) reveal the tides of RB to be of mixed diurnal and semidiurnal character, with two tides per day of unequal amplitudes during spring tides and two tides per day of nearly equal amplitudes during neap tides. Tidal ranges within the complex vary between 1.1 m during spring tides and 0.45 m during neap tides, corresponding to mean tidal prism of  $4.98 \times 10^6 \text{ m}^3$  for spring tides and  $3.84 \times 10^6 \text{ m}^3$  neap tides, respectively. While the tidal currents can be as strong as 1 m/s within narrow channel constrictions, they are generally much weaker over most of RB and HC.

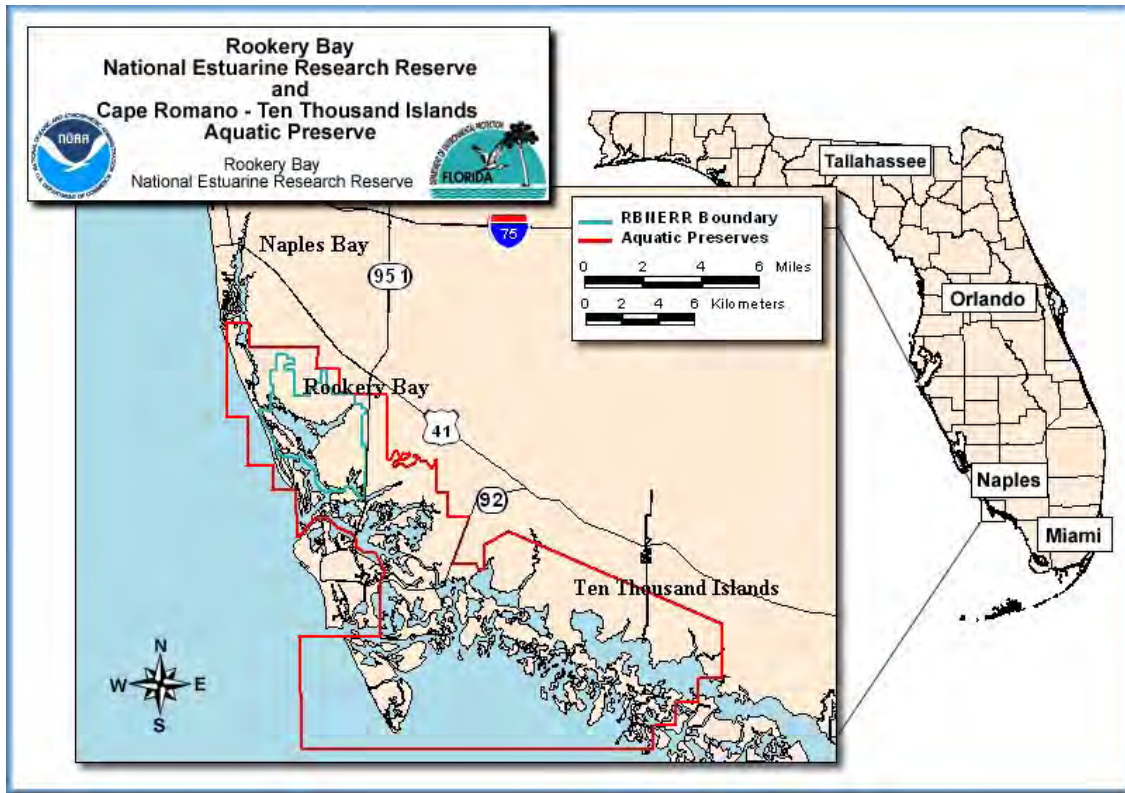


Fig. 1: Location of Rookery Bay and Henderson Creek

The rainfall and evaporation patterns for the region are categorized by Shirley et al., (2004). Average annual precipitation (rainfall) and evaporation over the RB estuary complex are estimated to be about 138 cm/yr and 120 cm/yr, respectively. Based on climatological averages the largest monthly rainfalls (20-23 cm/month) occur from June through October and the lowest monthly rainfalls (about 2-5 cm/month) occur from November through March (Shirley et al. 2004). These distributions give rise to classifications within four seasons as: 1) early dry (December through February), 2) late dry (March through May), 3) early wet (June through August), and 4) late wet (September through November). Along with local evaporation and precipitation are the freshwater inflows that occur primarily through HC at about 3 m<sup>3</sup>/s on annual average (Shirley et al., 2003). This discharge rate is related to the RB and HC estuary complex drainage basin rainfall, with the largest inflows occurring during the late wet season and lowest inflows occurring during the late dry season.

Seasonal salinity variations within the RB estuary complex occur primarily in response to the seasonal variations of net freshwater inflows (evaporation minus precipitation, plus stream inflows), with highest (lowest) salinity occurring in the late dry (wet) season. Daily salinity variations also occur in response to tides, with highest (lowest) salinity occurring at slack high (low) water. During the late dry season, and due to high evaporation and low precipitation rates, the salinity can exceed 40 psu. In contrast, during the late wet season, the salinity can be as low as 10 psu.

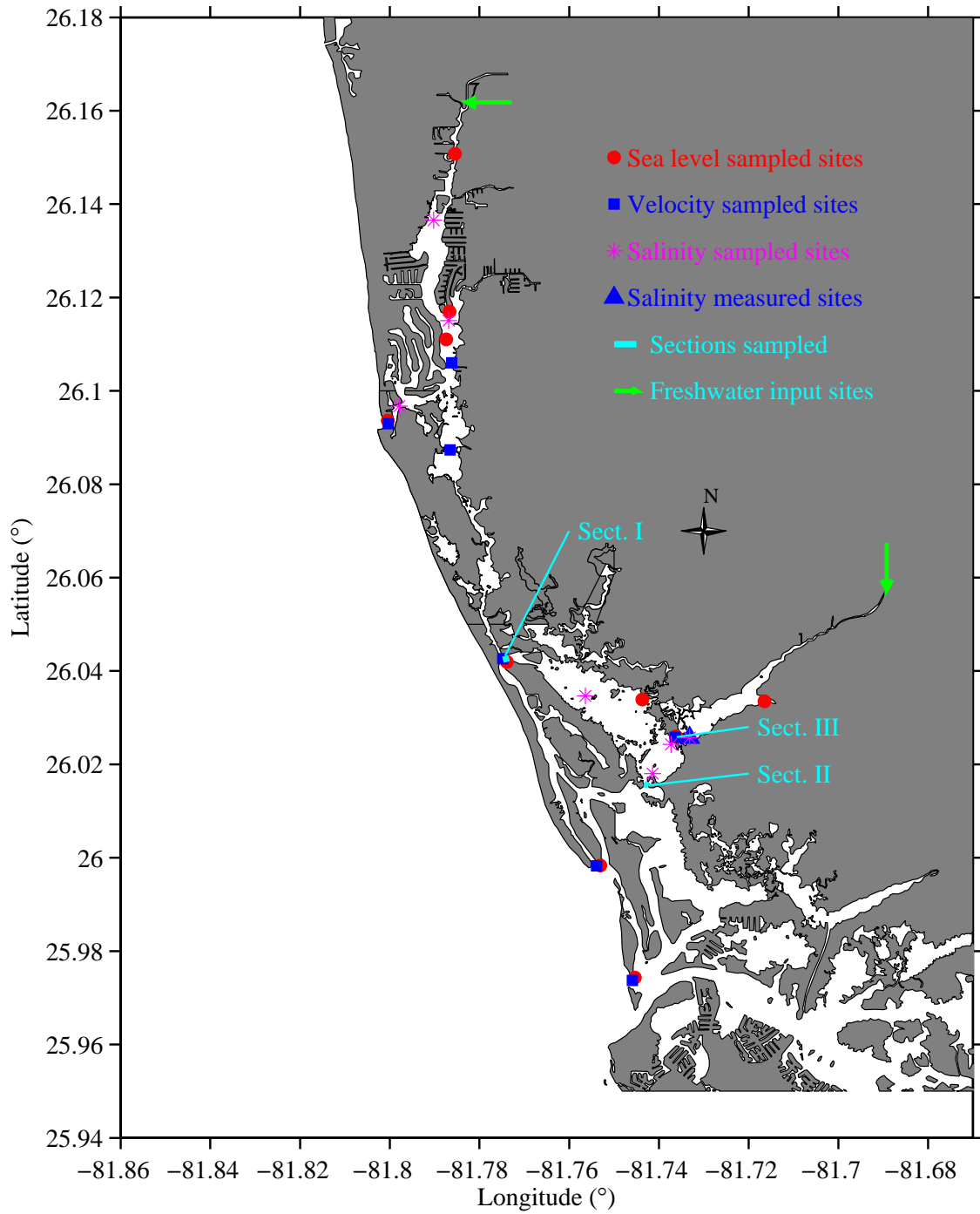


Fig. 2: Geometry of RB and HC estuary complex and the adjacent GOM shelf. The red filled circles denote the locations sampled model elevation. The blue filled squares denote the locations sampled model velocity. The magenta stars denote the locations sampled model salinity. The cyan lines (Sect. I, II and III) are used to calculate tidal water transports. The green vectors denote the locations of freshwater inflows.

Salinity variations play an important role in determining estuary habitat suitability for various fish and invertebrate species of sport and commercial value that impact tourism and other aspects of the local economy (Rubec et al., 2003; Shirley et al. 2004). For instance, a previous SFWMD project (Rubec et al., 2003) used habitat suitability modeling to relate different species life stages to the bottom salinity found in the RB estuary complex. The results suggest a causal link between spatial distributions of bottom salinity and species abundance over the course of various life stages. It is this causal linkage that necessitates a predictive capability for salinity distribution variations in response to fresh water inflow modifications, hence the justification of our studies from an environmental management point of view.

### **3. Description of the RB and NB estuary complex model**

Numerous 3D hydrodynamic models are available for application to the coastal oceans and estuaries. These include, but are not limited to the Princeton Ocean Model (POM) of Blumberg and Mellor (1987), the semi-implicit Estuarine, Coastal Ocean Model (ECOM\_si) of Blumberg (1993), the Regional Ocean Model System (ROMS) of Haidvogel et al. (2000), and the finite-element regional ocean model (QUODDY) (Lynch and Naimie, 1993). A recent development is the Finite Volume Coastal Ocean Model (FVCOM) of Chen et al. (2003) and applied to the Tampa Bay estuary by Weisberg and Zheng (2006). With regard to numerical discrete schemes, these models can be sorted into three categories: 1) finite-difference models (POM, ECOM\_si, and ROMS); 2) finite-element models (QUODDY); and 3) finite-volume models (FVCOM). The finite-difference models have the advantages of numerical simplicity and computational efficiency, whereas the finite-element models have the advantages of geometrical flexibility by virtue of unstructured triangular meshes that can accurately fit the irregular coastlines. The finite-volume model (FVCOM), employing a finite-difference discrete numerical scheme and a horizontal, non-overlapping unstructured triangular mesh, combines the best attributes of the finite-difference and finite-element methods. For the present RB estuarine complex modeling project, we chose the FVCOM to include the RB and NB estuary complex, inclusive of HC.

FVCOM uses a terrain following  $\sigma$ -coordinate in the vertical to better represent varying bottom topography. The 3D, primitive equations are solved by using a flux calculation integrated over each model grid control volume. This solution procedure facilitates the conservations of mass, momentum, energy, salt, and heat in both the individual control volumes and over entire the model domain. The FVCOM uses an upwind discretization scheme of second-order accuracy to calculate the advection terms in integral form over the control volume and a modified fourth-order Runge-Kutta scheme for integration in time. Because of its conservation characteristics, no temporal- or spatial-smoothing are required to stabilize the numerical computation. For computational efficiency the FVCOM solution consists of external and internal modes, each solved with distinctly different time steps, i.e., the external and internal mode time steps are set to accommodate the faster and slower barotropic and baroclinic responses, respectively. The external mode, composed of the vertically integrated momentum and continuity equations, solves for the surface elevation with a shorter time step, determined

by Courant-Friedrichs-Levy (CFL) numerical stability condition. The internal mode is a 3D and solves for the velocity, salinity, and temperature using a longer time step.

The model domain and the non-overlapping unstructured triangular grid used in this project are shown in Fig. 3. The model domain encompasses RB, Hall Bay, Johnson Bay, HC, Sand Hill Creek, Stopper Creek, NB, and a portion of the adjacent GOM shelf. To properly include tidal and wind forcing the model open boundary is located about 15 km away from the coast, arching from Doctors Pass in the north and Big Marco Island (BMI) in the south. The model grid consists of 34715 nodes and 63053 triangular cells in the horizontal and six evenly distributed  $\sigma$  levels in the vertical. Horizontal resolution increases from 150 m along open boundary to 18 m at the upstream of the HC.

With no bathymetry data for the RB estuary complex available in the NOAA estuarine bathymetry database, we collected the bathymetry data from different institutes and agencies, such as USF (Locker and Wright, 2003), FMRI (Dr. Rubec), and SFWMD (Mr. Liebermann), and we believe that the combined bathymetry dataset is now the most complete one for the RB estuary complex and NB. Figure 4 shows the combined bathymetry data over the model domain. Given the bathymetry and based on the CFL stability condition, the external and internal time steps chosen for the model are 0.4 s and 4 s, respectively.

The model is driven by tidal elevations along the open boundary, daily freshwater inflows from HC and Golden Gate (shown at Fig. 1), hourly winds, and daily evaporation and precipitation. The tidal elevations along the open boundary are specified by eight primary tidal constituents:  $M_2$ ,  $S_2$ ,  $N_2$ ,  $K_2$ ,  $O_1$ ,  $K_1$ ,  $P_1$ , and  $Q_1$ , sampled from our west Florida shelf (WFS) tide model (an unpublished refinement from He and Weisberg, 2002). The freshwater inflow rates, wind, and evaporation and precipitation rates are provided by RB National Estuaries Research Reserve (NERR) and SFWMD.

For comparative purposes we collected multiple-years of sea level data from NOAA-NOS tidal gauge at NB and performed a tidal harmonic analysis using the method of Foreman (1977). The harmonic constants of eight primary tidal constituents are given at Table 1. Similarly, to verify the salinity simulation, we collected multiple-years of salinity data observed at HC from RB NERR, the location of which is shown at Fig. 1.

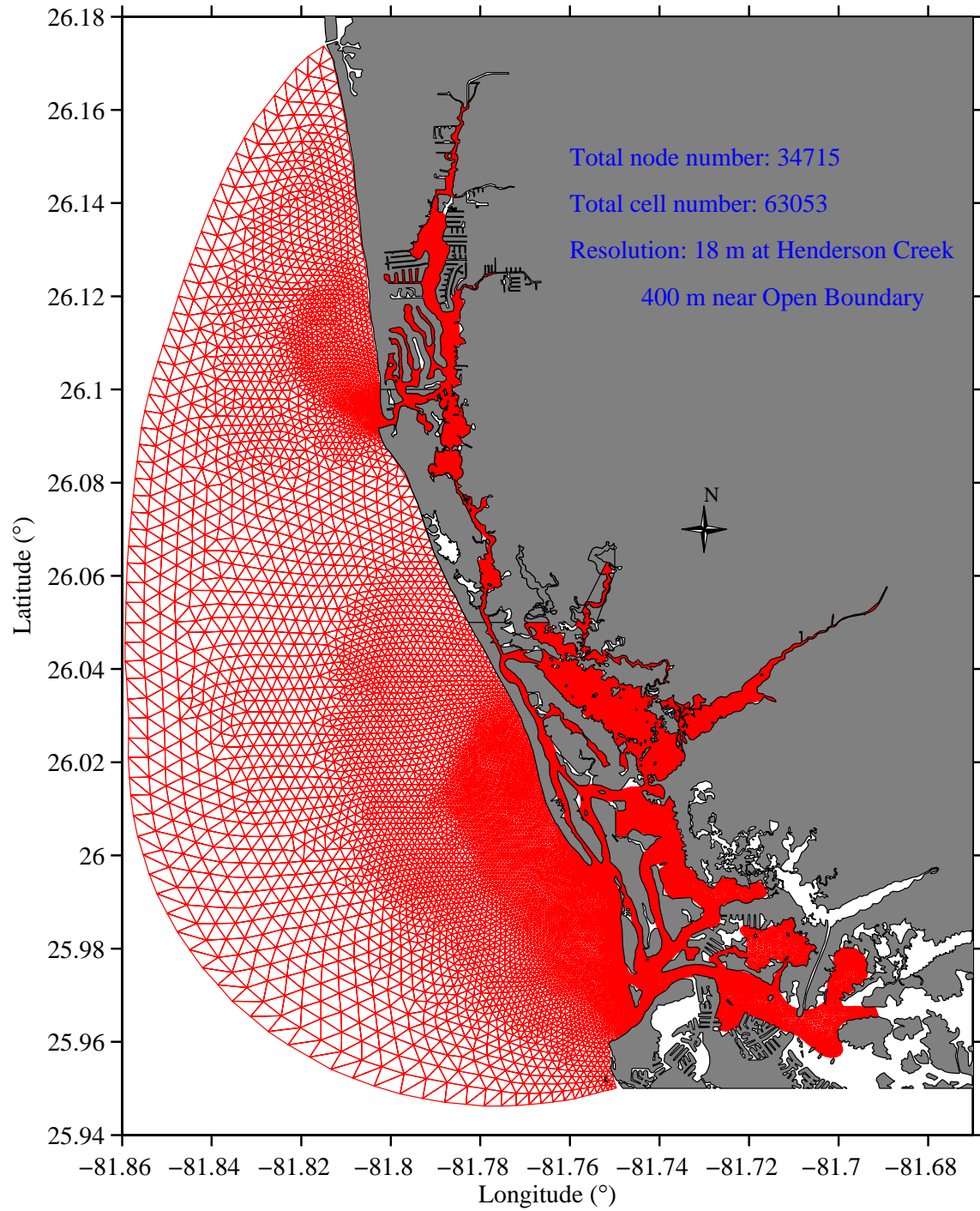


Fig. 3: The non-overlapping, unstructured triangular grid used in RB and NB estuary complex.

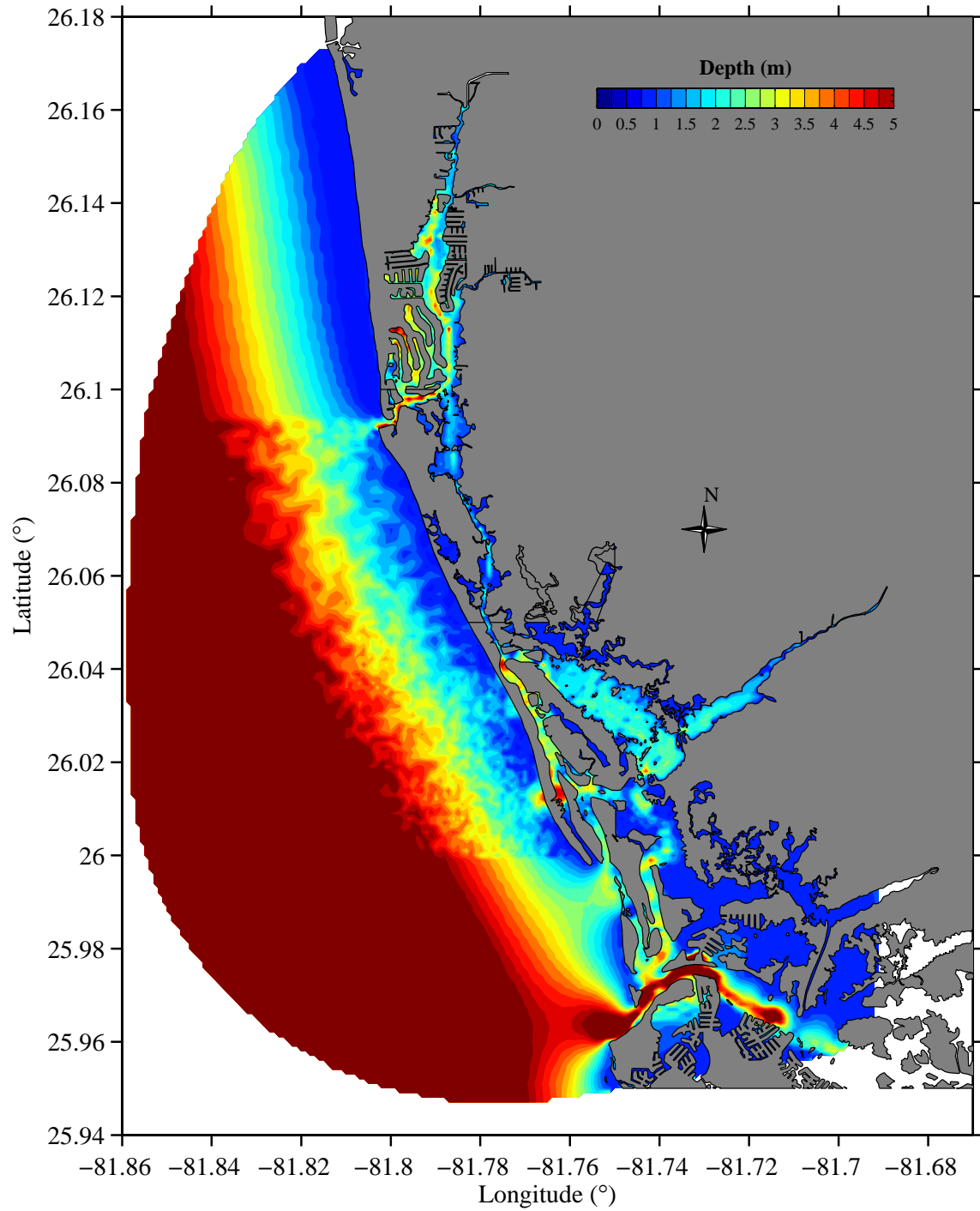


Fig. 4: Bathymetry of RB and NB estuary complex and the adjacent GOM shelf. Whereas high resolution bathymetry is available over much of the region the smooth looking regions are those for which we are limited to lower resolution NOAA bathymetric data.

#### 4. Tidal simulation

Since the water movement over the RB estuary complex is dominated by tides, we must first ensure a proper simulation of tides before we conduct the baroclinic salinity simulation. Previous WFS and Tampa Bay tidal simulation reveal that the eight primary tidal constituents ( $M_2$ ,  $S_2$ ,  $N_2$ ,  $K_2$ ,  $O_1$ ,  $K_1$ ,  $P_1$ , and  $Q_1$ ) account for more than 95% of the tidal variance over the entire WFS and its estuaries (He and Weisberg, 2002; Weisberg and Zheng, 2006). Thus the sea level along the open boundary is specified by combining these eight primary tidal constituents.

Table 1: Observed and modeled tidal amplitudes and phases of  $M_2$ ,  $S_2$ ,  $K_1$ ,  $O_1$ ,  $N_2$ ,  $K_2$ ,  $P_1$ , and  $Q_1$  and their differences at NB NOAA-NOS tidal gauge station.

| Tidal constituents | Observed |         | Modeled  |         | Difference |         |
|--------------------|----------|---------|----------|---------|------------|---------|
|                    | Amp (cm) | Pha (°) | Amp (cm) | Pha (°) | Amp (cm)   | Pha (°) |
| $M_2$              | 26.35    | 143.1   | 26.07    | 144.5   | -0.28      | 1.4     |
| $S_2$              | 8.90     | 154.3   | 8.27     | 155.1   | -0.63      | 0.8     |
| $K_1$              | 15.23    | 8.9     | 15.55    | 10.6    | 0.32       | 1.7     |
| $O_1$              | 13.64    | 3.0     | 13.68    | 4.0     | 0.04       | 1.0     |
| $N_2$              | 5.47     | 129.7   | 5.31     | 130.4   | -0.16      | 0.7     |
| $K_2$              | 2.47     | 144.3   | 2.68     | 125.6   | 0.21       | -18.7   |
| $P_1$              | 5.17     | 8.0     | 4.61     | 10.0    | -0.56      | 2.0     |
| $Q_1$              | 3.11     | 351.8   | 3.14     | 353.4   | 0.03       | 1.6     |

##### 4.1. Comparisons between modeled and observed sea level

To resolve the spring-neap tidal cycle, the model was run for 65 days which the first 5 days are the model ramp-up and the additional 60 days is used for model analysis. The eight primary tidal constituents are separated from the model-simulated surface elevation by using linear least squares harmonic analysis method of Foreman (1977). A direct comparison between modeled and observed amplitudes and phases of eight tidal constituents at NB is given at Table 1. Modeled amplitudes and phases for eight primary tidal constituents are in good agreement with observational data at NB tidal gauge station. The differences between the modeled and observed amplitudes and phases are less than 1 cm and 2°, respectively, except for semi-diurnal  $K_2$  tide which the modeled and observed tidal phase difference is 18.7°. However, the amplitude of  $K_2$  tide is smallest among the eight tidal constituents, which implies that even though there is large phase difference for  $K_2$  tide, its small amplitude has only small effect on the total elevation, which is obvious

in Fig. 5. The model also shows agreeable with observations in the simulation of fortnightly and monthly spring-neap tide variation. Figure 5 shows the comparison between modeled (blue) and observed (black) tidal elevations, constructed from the eight primary tidal constituents, over a 1 month period at the NB NOAA tide station. Since there are no current observations available within the RB and NB estuary complex, we are limited in our comparisons to elevations at NB tidal station. This comparison demonstrates the legitimacy of the open boundary condition used in forcing the tides.

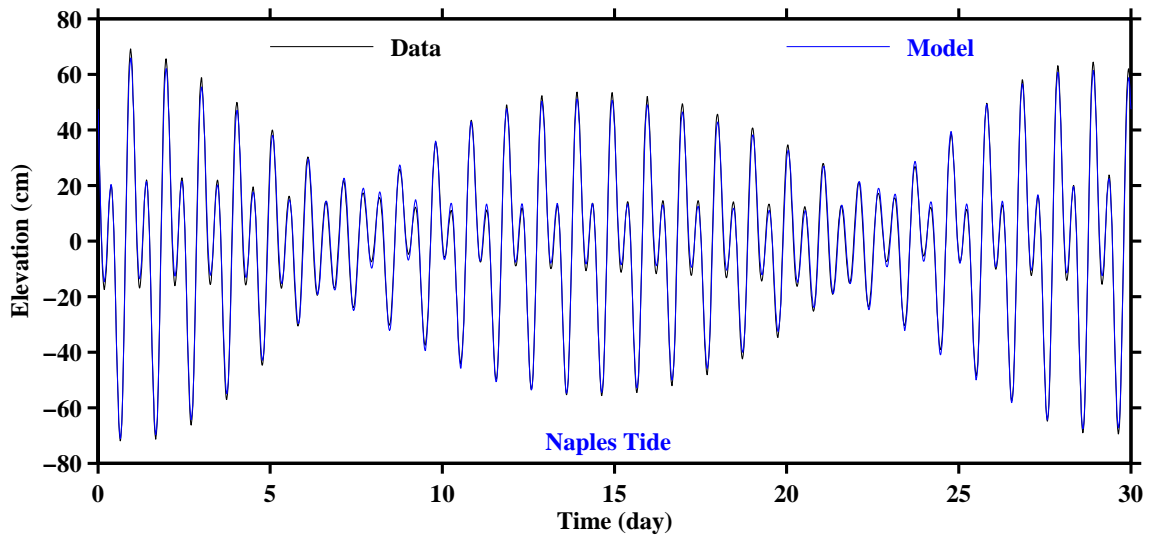


Fig. 5: Comparisons between modeled (blue) and observed (black) tidal elevation at NB NOAA-NOS tidal gauge station over a one month period. The elevations are constructed based on the summations of eight primary tidal constituents ( $M_2$ ,  $S_2$ ,  $K_1$ ,  $O_1$ ,  $N_2$ ,  $K_2$ ,  $P_1$ , and  $Q_1$ ).

#### 4.2. Tidal elevation

Model-predicted sea level variations over a two month period sampled within the RB (HC, Hall Bay, Stopper Creek, and Holloway Island) and NB (Gordon Pass, Dollar Bay, upper NB, and middle NB) estuary complex, and along the coast [BMI and Little Macro Island (LMI)] are presented at Fig. 6. Here in this report we will focus our discussion on the RB estuary complex since NB was not part of our original proposal. The tidal variations over the RB estuary complex and the adjacent coast show the mixed semi-diurnal and diurnal character, with two high and low tides per day of unequal amplitudes during spring tides and two high and low tides per day of nearly equal amplitudes during neap tides, consistent with observation made by Lee and Yokel (1973). When the tides propagate across the GOM shelf and into RB complex through the two narrow and shallow inlets, the bottom friction and lateral dissipation cause the sea elevation decrease, particular during spring tides when the current speeds are larger, causing more energy to be dissipated by larger bottom friction and lateral dissipation. For instance, during the spring tides, the tidal ranges are 1.3 m at BMI, 0.95 m at Holloway Island, and 0.8 m at Hall Bay, respectively, whereas during the neap tides, the tidal ranges are 0.45 m at BMI, 0.4 m at Holloway Island, and 0.35 m at Hall Bay, respectively. Our modeled tide ranges during spring and neap tides are different from

findings by Lee and Yokel (1973) which stated tidal range are 1.1 m during spring tides and 0.45 m during neap tides, respectively. The differences can be attributed to the effects of wind and freshwater inflow on the observations that are not included in the tidal simulation. When these effects are taken into account, the model-predicted tidal ranges over the RB estuary complex and the adjacent GOM coast are in good agreement with the observation.

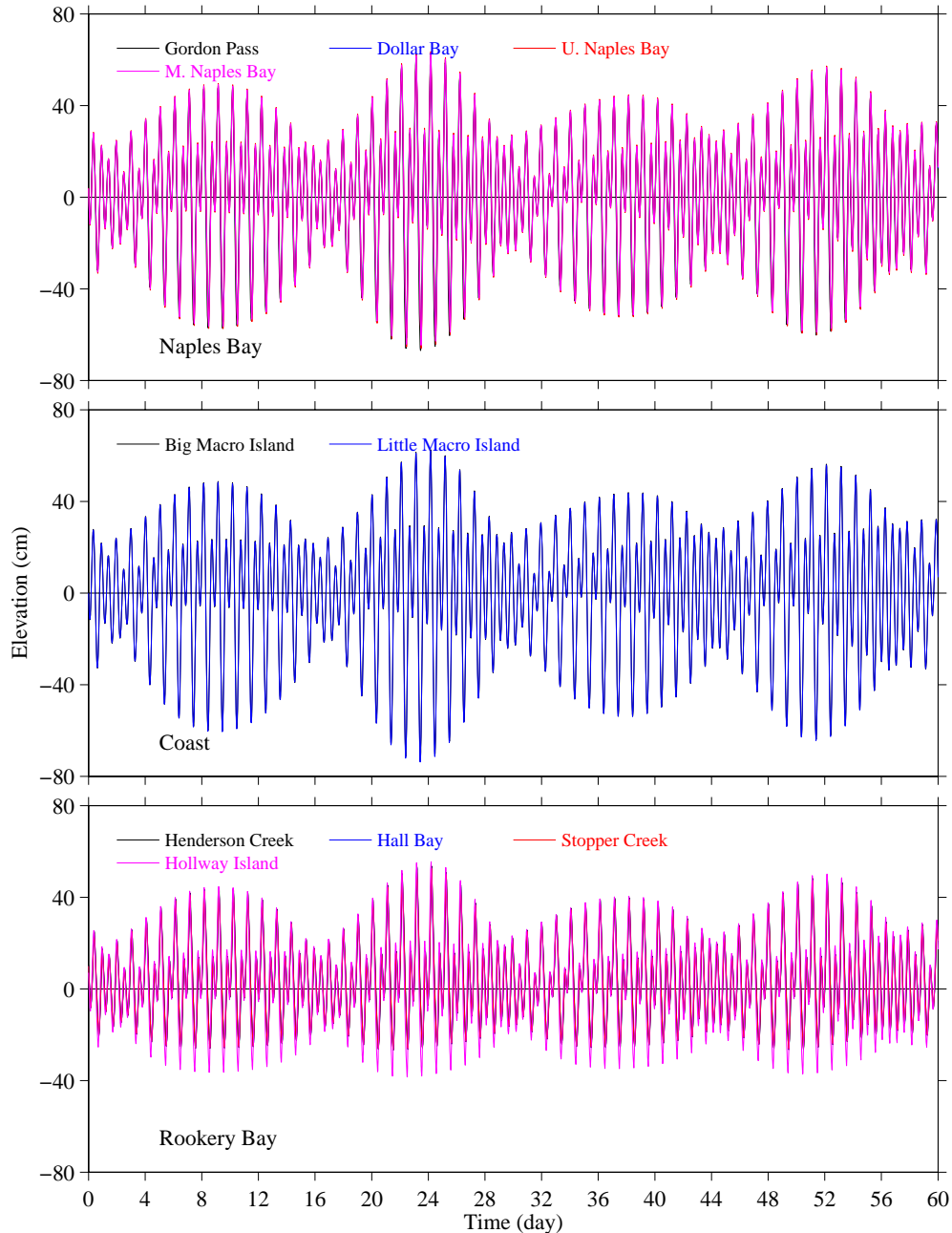


Fig. 6: Model-predicted tidal elevations over a two months period sampled at RB and HC estuary complex (lower), GOM coast (middle), and NB (upper). The locations are shown at Fig. 1.

Table 2 provides the tidal harmonic constants for the four principal tidal constituents ( $M_2$ ,  $S_2$ ,  $O_1$ , and  $K_1$ ) sampled over the RB estuary complex and the adjacent GOM coast. Over the RB estuary complex (HC, Hall Bay, and Stopper Creek), the tidal amplitudes are almost identical and the phase differences are less than  $6^\circ$ , which is about 12 minutes for semi-diurnal tides or 24 minutes for diurnal tides. This implies that the sea level over the entire RB estuary complex basin rises and falls almost simultaneously. From the GOM coast to RB complex, the tidal amplitudes decrease by about 12 cm for  $M_2$  tide, 4 cm for  $S_2$  tide, 3.5 cm for  $O_1$  tide, and 5 cm for  $K_1$  tide, and the tidal phases lag by  $60^\circ$  (or 2 hours) for  $M_2$  tide,  $70^\circ$  (or 2.3 hours) for  $S_2$  tide,  $55^\circ$  (or 3.7 hours) for  $O_1$  tide, and  $50^\circ$  (or 3.3 hours) for  $K_1$  tide, respectively.

Table 2: Model-predicted tidal amplitudes (cm) and phases ( $^\circ$ ) of 4 principal tidal constituents ( $M_2$ ,  $S_2$ ,  $O_1$ , and  $K_1$ ) at RB and HC estuary complex (HC, Hall Bay, Stopper Creek, and Holloway Island) and the adjacent GOM coast (BMI and LMI).

| Location        | $M_2$ |       | $S_2$ |       | $O_1$ |      | $K_1$ |      |
|-----------------|-------|-------|-------|-------|-------|------|-------|------|
|                 | Amp.  | Pha.  | Amp.  | Pha.  | Amp.  | Pha. | Amp.  | Pha. |
| HC              | 15.15 | 202.4 | 4.52  | 226.7 | 10.15 | 57.9 | 10.63 | 60.9 |
| Hall Bay        | 15.09 | 199.1 | 4.47  | 222.6 | 10.08 | 55.8 | 10.60 | 58.7 |
| Stopper Creek   | 15.11 | 198.2 | 4.47  | 221.4 | 10.07 | 55.6 | 10.57 | 58.5 |
| Holloway Island | 19.25 | 174.3 | 5.84  | 191.5 | 10.85 | 34.8 | 11.79 | 37.9 |
| BMI             | 27.17 | 143.6 | 8.68  | 154.9 | 13.73 | 3.17 | 15.61 | 9.9  |
| LMI             | 27.44 | 140.6 | 8.74  | 150.7 | 13.73 | 1.0  | 15.70 | 7.8  |

### 4.3. Tidal current

Model-predicted tidal currents over two month period, sampled at Hall Bay, BMI, Hurricane Pass, Holloway Island, Dollar Bay, Gordon Pass, and Middle Naples Bay, are presented at Fig. 7. Similar to the sea elevation variations, the tidal currents exhibit fortnightly and monthly spring-neap tidal cycle as well. During the spring tides, the current velocity is found about 0.7 m/s at BMI and 0.4 m/s over the Hall Bay, whereas during the neap tides, they decrease to 0.2 m/s at both locations. Table 3 provides tidal ellipse parameters (major axis, minor axis, orientation of the major axis, and the times of maximum current) for four principal tidal constituents ( $M_2$ ,  $S_2$ ,  $O_1$ , and  $K_1$ ) over the RB estuary complex and the adjacent GOM coast. The maximum ratio of minor axis to major axis is 0.1 and the orientations of four tidal constituents are almost the same at each sampled location, indicating that the tidal currents over the RB estuary complex are rectilinear. The tidal currents rotate clockwise over the entire complex.

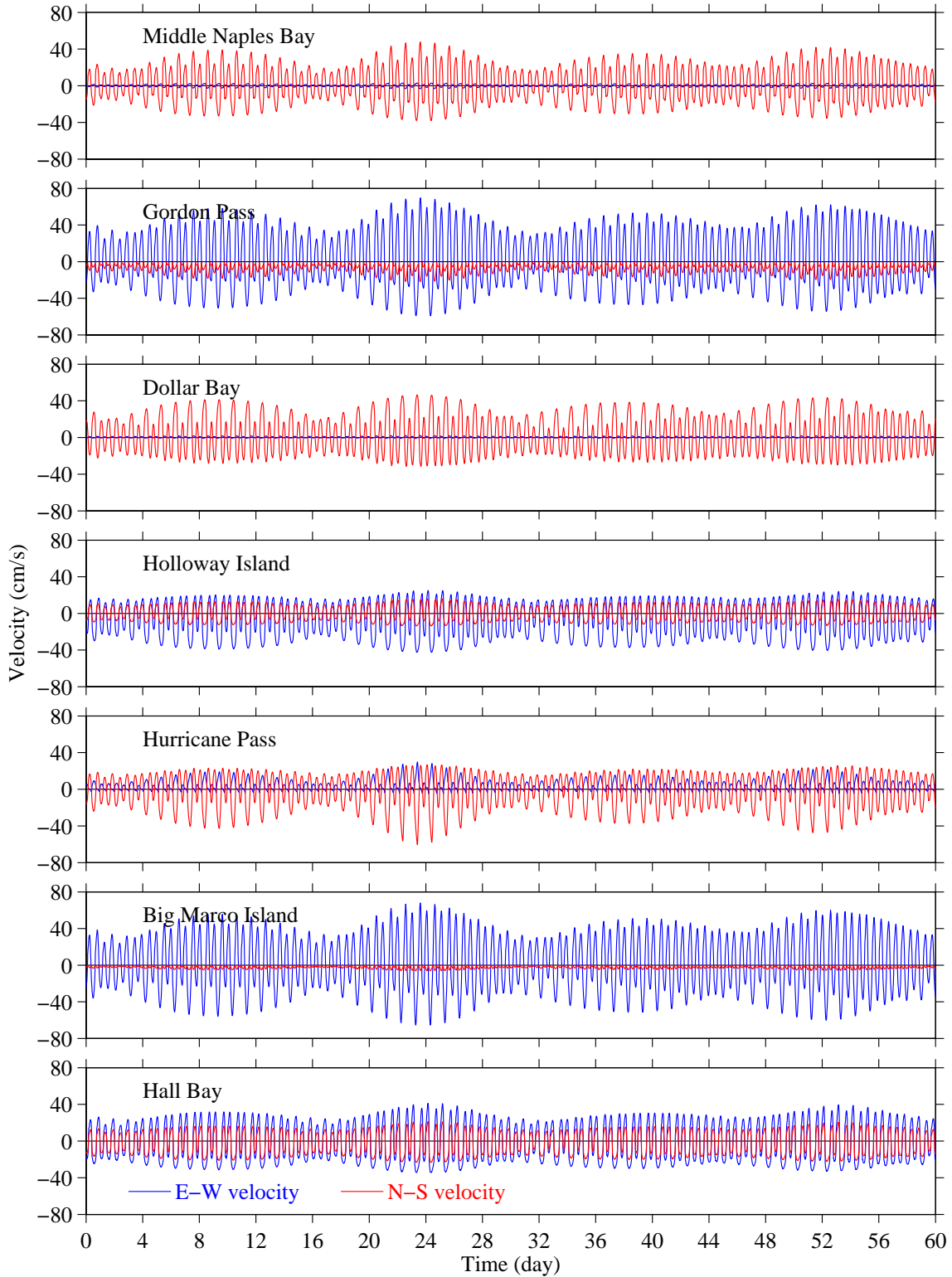


Fig. 7: Model-predicted tidal current velocities over a two months period sampled at Hall Bay, BMI, Hurricane Pass, Holloway Island, Dollar Bay, Gordon Pass, and middle NB (from lower to upper). The locations are shown at Fig. 1. The blue and red lines denote eastward and northward components of current vectors.

Table 3: Model-predicted tidal current parameters of four principal tidal constituents ( $M_2$ ,  $S_2$ ,  $O_1$ , and  $K_1$ ) at RB (Hall Bay and Holloway Island) and the GOM coast (BMI and Hurricane Pass).  $U_{\text{major}}$  = amplitude of the major axis;  $U_{\text{minor}}$  = amplitude of the minor axis;  $\theta_{\text{orien}}$  = orientation of the major axis;  $G$  = time of maximum current (Greenwich phase in degree,  $1^\circ = 2$  minutes for  $S_2$  tide and 2.07 minutes for  $M_2$  tide). The orientation is measured counterclockwise from the east. The negative sign in the  $U_{\text{minor}}$  indicates a clockwise rotation of current vectors.

| Location        | Tide  | $U_{\text{major}}$ (cms <sup>-1</sup> ) | $U_{\text{minor}}$ (cms <sup>-1</sup> ) | $\theta_{\text{orien}}$ (°) | $G$ (°) |
|-----------------|-------|---|---|-----------------------------|---------|
| Hall Bay        | $M_2$ | 28.4                                    | -0.2                                    | 30.5                        | 115     |
|                 | $S_2$ | 8.80                                    | -0.01                                   | 30.4                        | 140     |
|                 | $O_1$ | 9.52                                    | -0.08                                   | 31.8                        | 148     |
|                 | $K_1$ | 10.84                                   | -0.06                                   | 31.6                        | 151     |
| BMI             | $M_2$ | 37.96                                   | -0.25                                   | 0.0                         | 63      |
|                 | $S_2$ | 12.22                                   | -0.06                                   | 0.2                         | 78      |
|                 | $O_1$ | 9.19                                    | -0.01                                   | 2.3                         | 107     |
|                 | $K_1$ | 11.36                                   | -0.10                                   | 2.4                         | 111     |
| Hurricane Pass  | $M_2$ | 22.15                                   | -2.21                                   | 102.4                       | 95      |
|                 | $S_2$ | 7.01                                    | -0.69                                   | 102.4                       | 112     |
|                 | $O_1$ | 8.66                                    | -0.22                                   | 109.0                       | 132     |
|                 | $K_1$ | 9.55                                    | -0.48                                   | 108.1                       | 140     |
| Holloway Island | $M_2$ | 23.77                                   | -2.1                                    | 23.7                        | 120     |
|                 | $S_2$ | 7.27                                    | -0.78                                   | 23.1                        | 143     |
|                 | $O_1$ | 9.26                                    | -0.49                                   | 19.3                        | 151     |
|                 | $K_1$ | 10.42                                   | -0.66                                   | 19.6                        | 155     |

Figures 8-9 show the synoptic distributions of the model-predicted near surface tidal current vectors at maximum flood and ebb tidal phases during spring tides and Figs. 10-11 are for neap tides. The tidal current over the RB estuary complex is small with less than 0.2 cm/s except at the narrow channels. The maximum tidal current with speed greater than 1.2 m/s is found at the channel connecting Johnson Bay and RB during the spring tides. During the neap tides, the maximum current is about 1 m/s at this location.

#### 4.4. Tidal volume transports

To quantitatively estimate the water volume transports between RB complex and the GOM shelf through sections I and II (shown at Fig. 1) and between RB and HC through section III, we calculate the water volume transports  $Q$  as:

$$Q = \int_0^T \int_0^L \int_0^h \vec{V} \cdot \vec{n} dx dz dt$$

where  $T$  is the tidal cycle,  $L$  is the width of section,  $h$  is the depth,  $\vec{V}$  is the current vector, and  $\vec{n}$  is the normal vector to the section.

The tidal volume transports for the flood and ebb phases during spring and neap tides through the three selected sections are given in Table 4. The total flood volume entering RB complex is about  $4.73 \times 10^6 \text{ m}^3$  during spring tides and  $2.32 \times 10^6 \text{ m}^3$  during

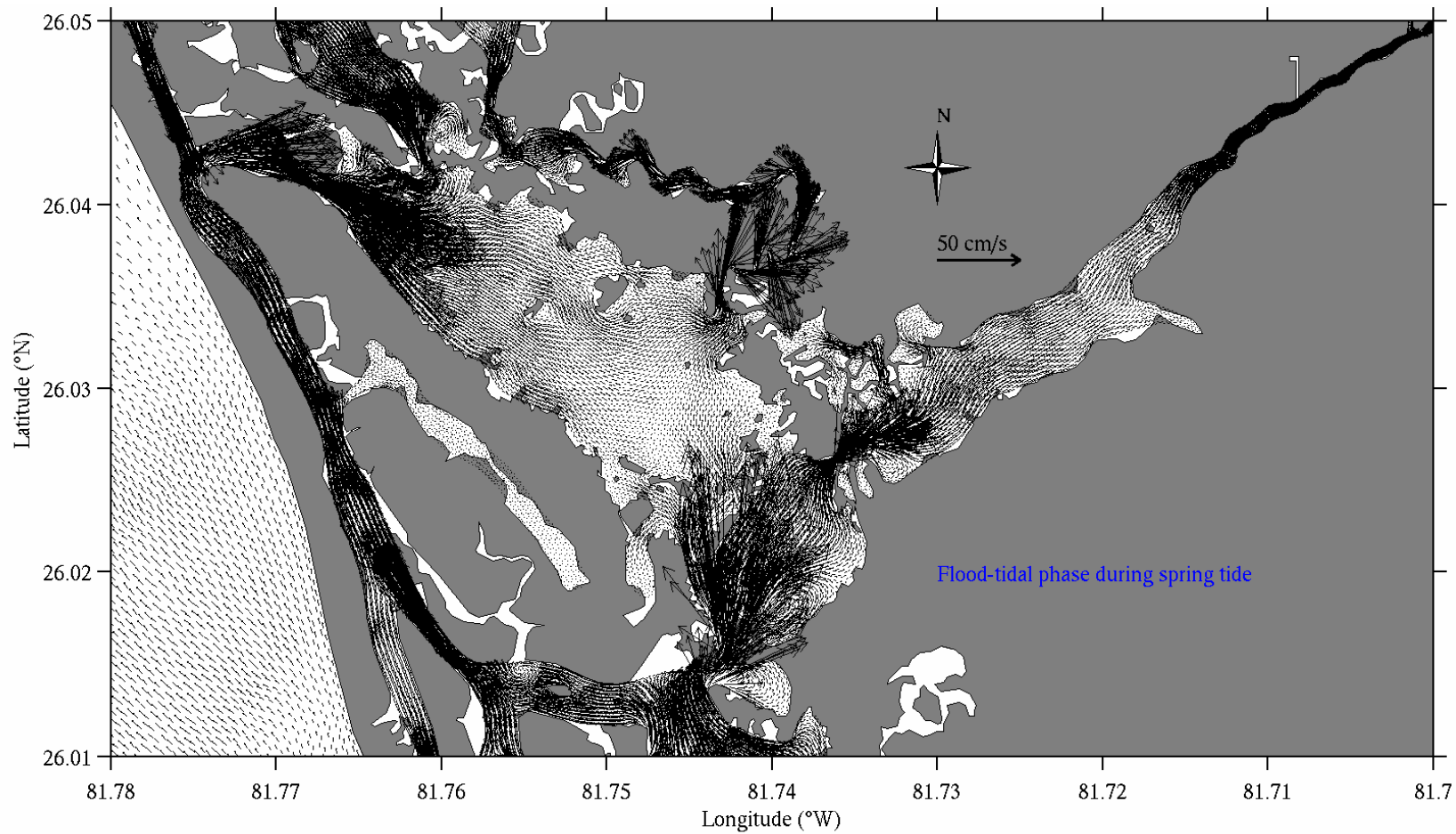


Fig. 8: Synoptic distributions of the near surface tidal current vectors at maximum flood tidal phase during the spring tides.

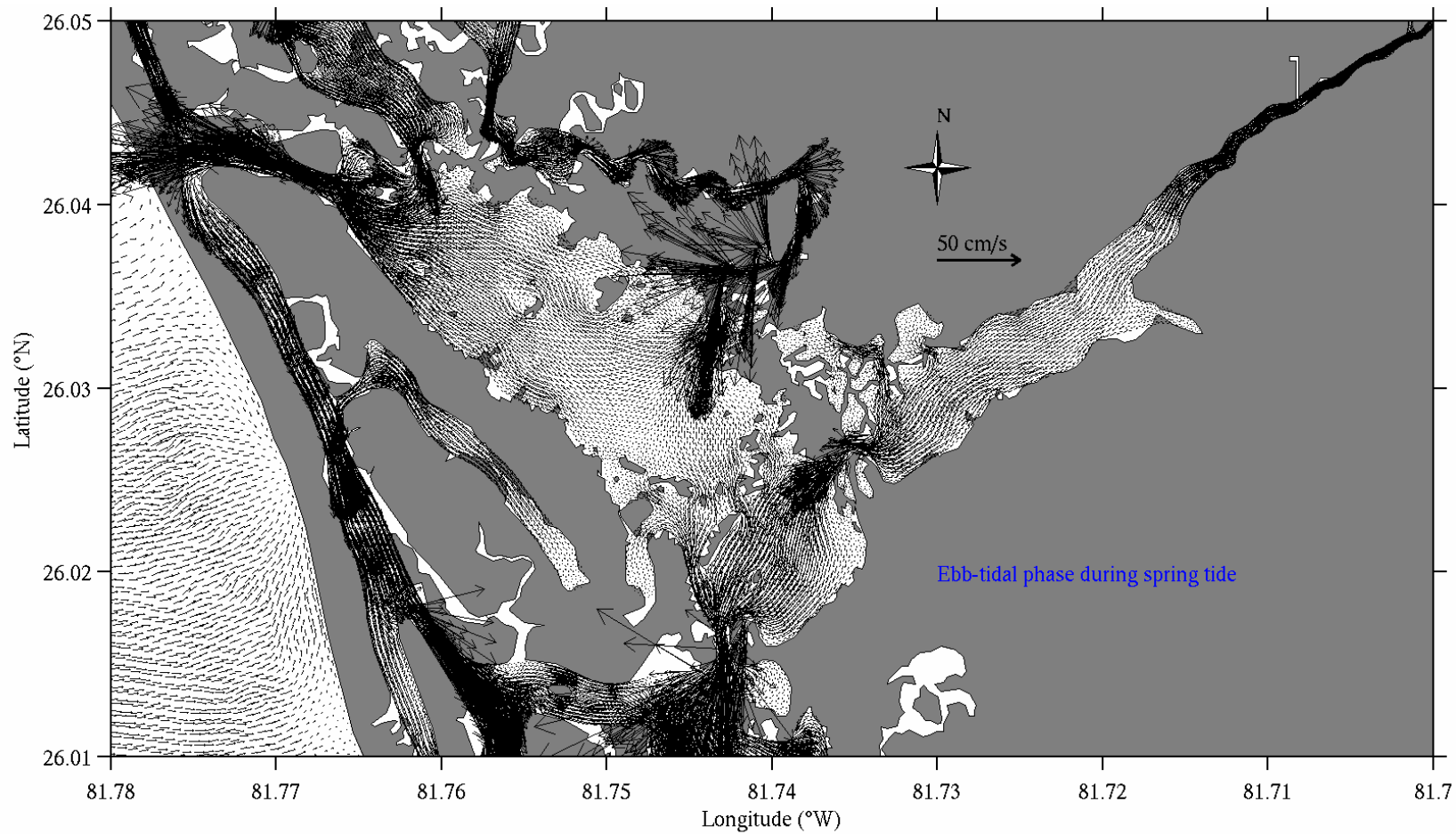


Fig. 9: Same as Fig. 8, except at the maximum ebb tidal phase.

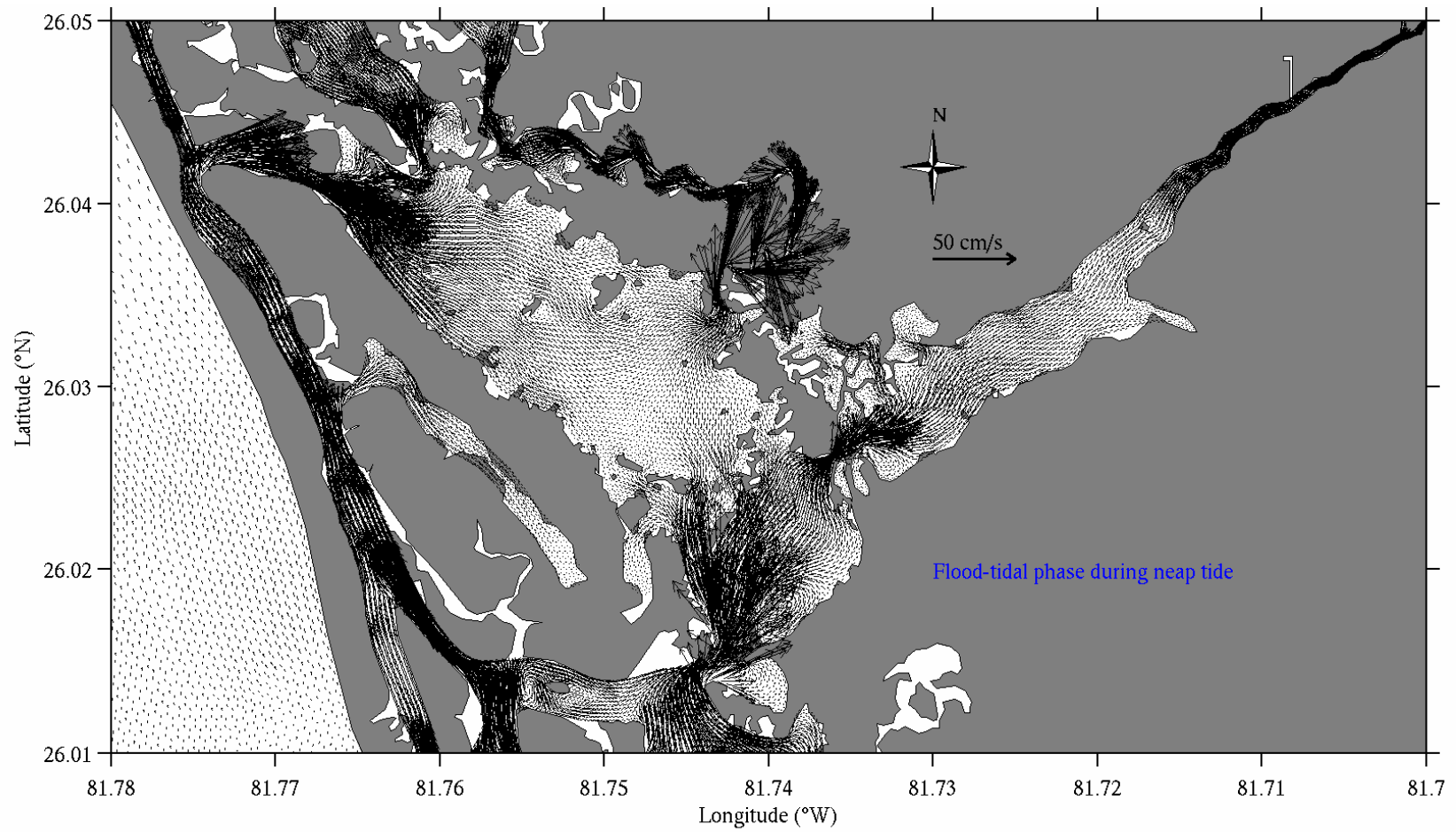


Fig. 10: Same as Fig. 8, except during the neap tides.

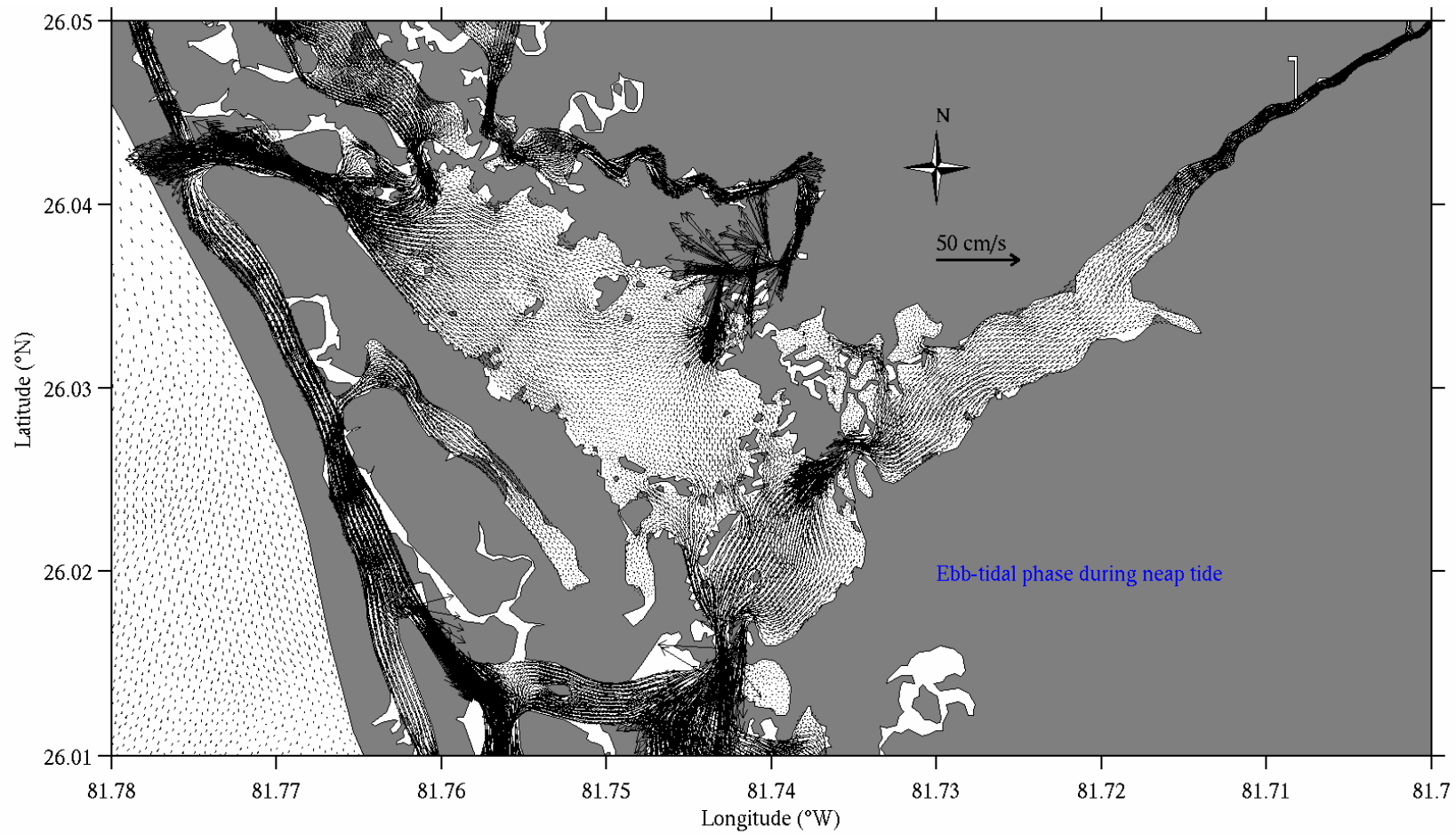


Fig. 11: Same as Fig. 9, except during the neap tides.

neap tides, where 55% through inlet connecting Johnson Bay (section II) and the other 45% through northwest channel (section I). 20% of flood volume entering RB complex enters HC through section III. Our model result is different from Lee and Yokel (1973) which stated 75% of flood volume entering RB complex passes through section II and the other 25% though northwest inlet. The difference might be related to 1) the coastline and bathymetry changes after 1973 and 2) only one current measurement was made at each section to estimate volume transport. Since we use updated coastline and bathymetry data and have much high spatial and temporal resolution of current (at least 3 points at each section, 5 points in the vertical, and output each 5 minutes), we believe our results present the realistic volume transports entering RB complex.

Table 4: Tidal water transports between GOM shelf and RB complex (sum of sections I and II) and between RB and HC (section III) during spring and neap tides.

|              | Sect. I            |                    | Sect. II           |                    | Sect. III          |                    |
|--------------|--------------------|--------------------|--------------------|--------------------|--------------------|--------------------|
|              | Flood              | Ebb                | Flood              | Ebb                | Flood              | Ebb                |
| Spring tides | $2.18 \times 10^6$ | $2.51 \times 10^6$ | $2.55 \times 10^6$ | $3.04 \times 10^6$ | $1.17 \times 10^6$ | $1.18 \times 10^6$ |
| Neap tides   | $1.13 \times 10^6$ | $1.13 \times 10^6$ | $1.19 \times 10^6$ | $1.30 \times 10^6$ | $0.54 \times 10^6$ | $0.54 \times 10^6$ |

## 5. Salinity simulations

Based on the success of the tidal simulation, we added forcings of freshwater inflows, precipitation, evaporation, and wind to conduct a salinity simulation. There are four fresh water inflows to HC and RB: the Hwy. 41 canal (main weir #1), the Hwy. 951 canal, Eagle Creek, and the Lely canal, with the first three entering HC and the last entering RB (M. Shirley, personnel communication). Our understanding is that the primary inflow is via the main weir #1 and through the present time this is the only fresh water inflow data that has been supplied to us by SFWMD. We performed our salinity simulation experiments for 2005 since this was the most recent time period for which we had observed fresh water inflow (from SFWMD) and salinity data (from RBNERR) along with winds, precipitation, and evaporation data also from SFWMD.

Figure 12 shows the observed salinity, freshwater inflow, wind, precipitation, and evaporation data for 2005. The salinity show seasonal variation depending on freshwater inflow variations, as well as daily variation depending on tidal current variation. During the first half year (early dry and late dry seasons), the salinity exhibits small variation with value of more than 30 psu because the freshwater inflow is very small. After June 1, the rainfall increases and the freshwater inflows significantly increase, leading to salinity decreasing to below 10 psu at the end of June when the freshwater inflow is more than  $250 \text{ ft}^3/\text{s}$ . The evaporation rate shows small perturbation. The wind is weak during winter and strong during fall which might be related to the passing of hurricanes. For instance, the 20 m/s northeastern wind is found on October 24 when the hurricane Wilma made landfall at the south of RB complex.

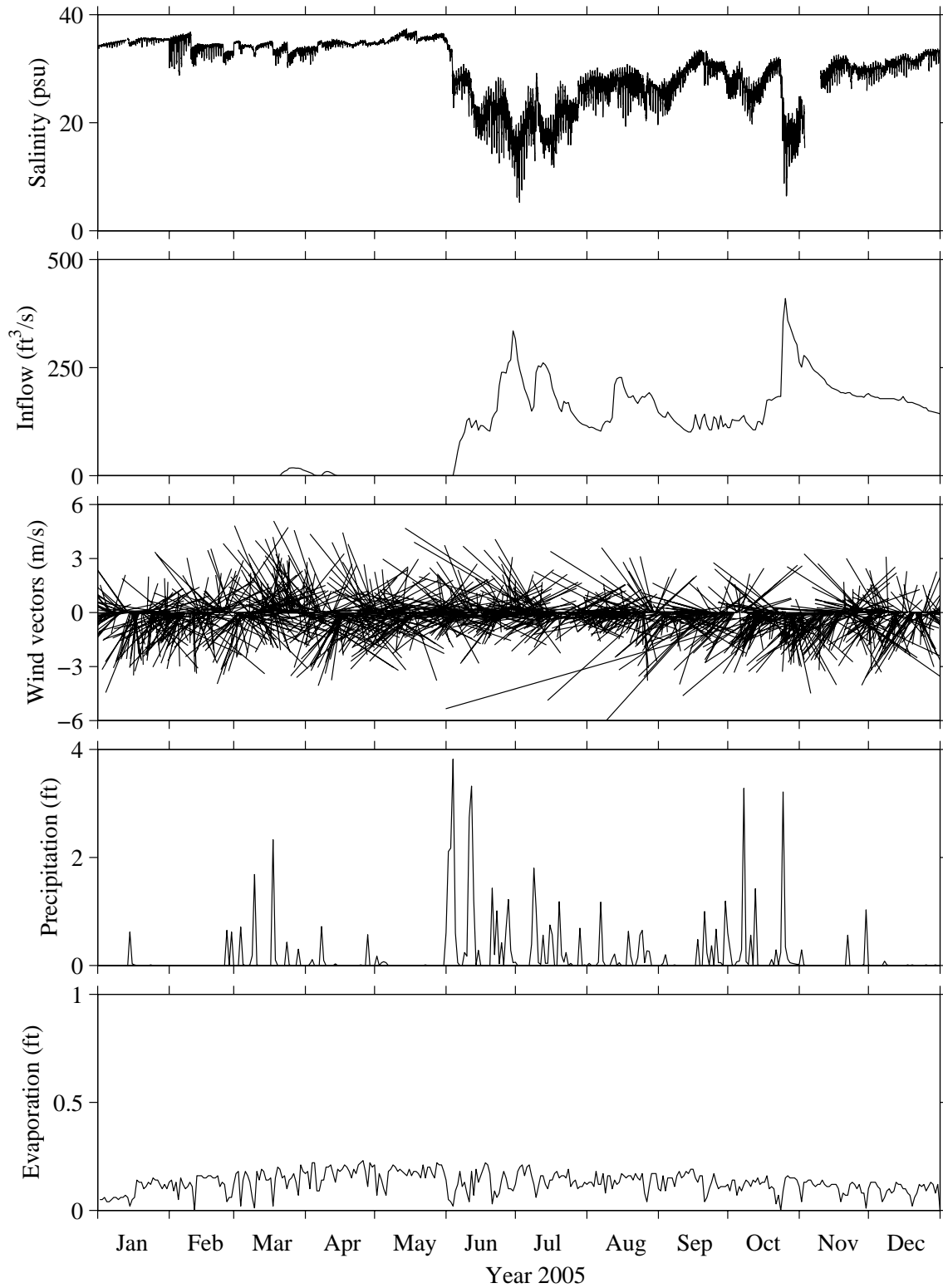


Fig. 12: Panels from up to down represent the time series of measured salinity in HC, freshwater inflow to HC, wind vectors, precipitation, and evaporation over the RB complex in 2005.

Due to the large number of model grid points and small time step, computer limitations allowed for two separate experiments: one for the early wet season (beginning June 1) and the other for the late wet season (beginning September 1). For each of these the initial salinity is specified as 36 psu and the model was run for 60 days, the first 20 days of which was used for the initial salinity equilibration time. Here we define the equilibration time as the time necessary for the fresh water inflow to permeate the entire estuary complex such that the subsequent variations in salinity are due to external factors and not just the initial spreading of fresh water throughout the estuary. For the early and wet season model runs, the comparisons of modeled and observed salinity along with the wind, evaporation, precipitation, river inflow forcing functions, and the model and sea level fluctuations inside HC are shown in Figs. 13 and 14, respectively. The model-predicted salinity at HC is in reasonable agreement with observations in both seasons. In both cases there is a general agreement in the tidal and longer term variations. There are discrepancies, however, and it is unclear whether these result from inadequacies in the fresh water inflows or the evaporation and precipitation estimates. It is important to point out here that even a perfect model with zero error (such as a closed form analytical solution to a set of equations) will have variations based on the boundary conditions (here the forcing functions of rivers, tides, winds, precipitation and evaporation). With the model veracity at times being very good we suspect that the mismatches between the salinity simulations and the data when these occur are more the result of inadequate forcing functions than they are model performance. In other words, improved fresh water inflow rates from all possible sources (we were only supplied with weir #1) should lead to improved results. Nevertheless the results obtained look very good.

## **6. Scenario experiments**

One of the environmental management goals of this project is to be able to relate the HC freshwater inflows to the salinity pattern variations over the entire RB estuary complex. While beyond the scope of the original proposal we accelerated our performance at the request of Ananta Nath, SFWMD to run two different fresh water inflow scenario experiments as a precursor to future environmental management applications. The results supplied to SFWMD are repeated here.

### **6.1. Scenario 1**

In this scenario, some amount of fresh water is diverted from the Golden Gate canal and deposited into HC through the main weir #1 during the late wet season. The discharge rates of diversion are 50 ft<sup>3</sup>/s or 100 ft<sup>3</sup>/s. To simulate the potential effects of such flow modification we ran three separate simulations for the period September 1 through December 31, 2005: 1) using the realistic discharge rates collected from SFWMD [S1]; 2) adding 50 ft<sup>3</sup>/s to these realistic discharge rates [S2]; and 3) adding 100 ft<sup>3</sup>/s to these realistic discharge rates [S3]. Other forcings (tidal elevation along the open boundary, surface wind, precipitation, and evaporation) are the same for these three experiments.

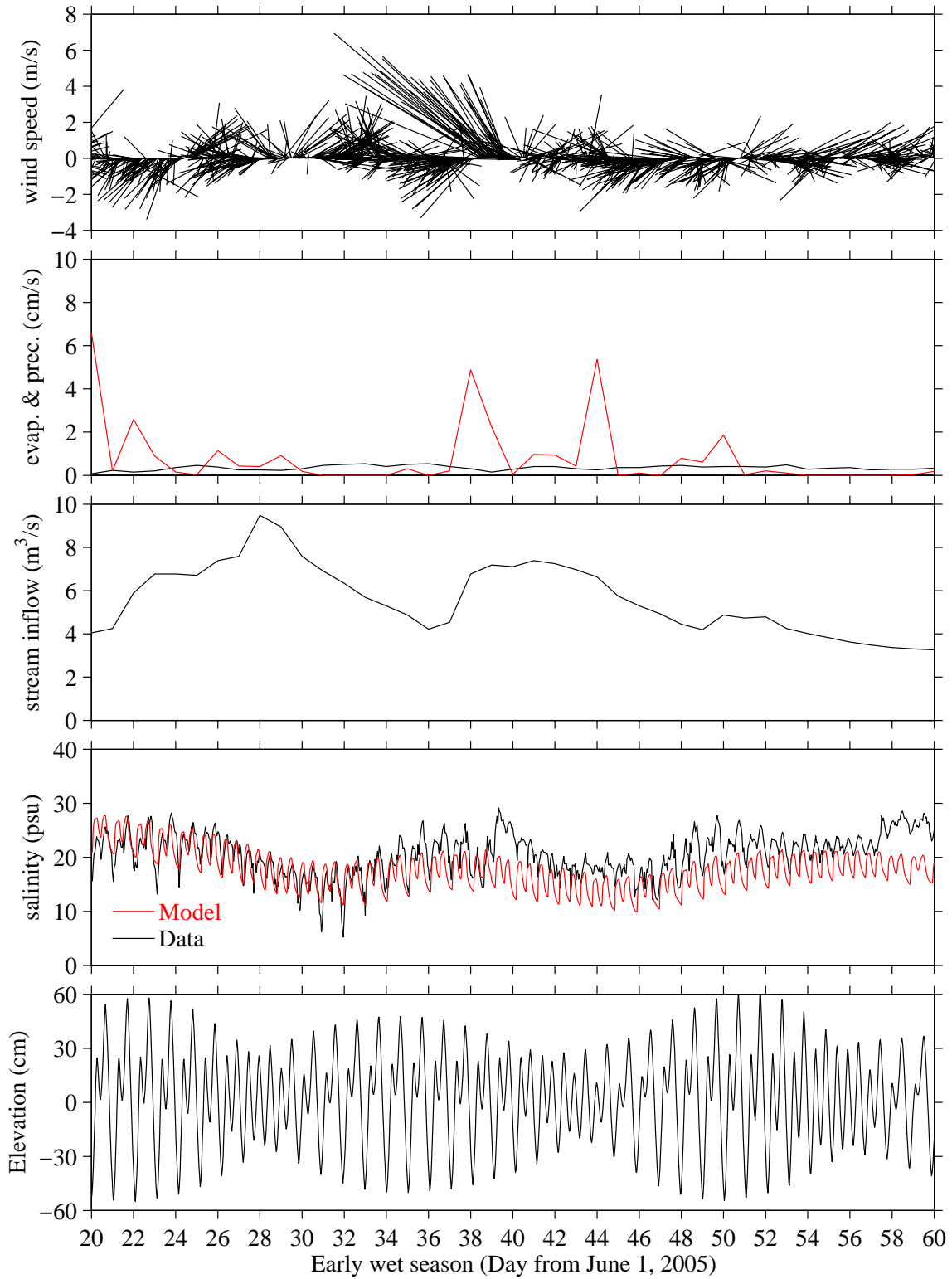


Fig. 13: Panels from up to down represent the model input of winds, precipitation (red) against evaporation (black), stream inflow at hwy 41, model output salinity (red) and observed salinity (black) at HC, and model output sea level in HC for early wet season period of June 20 through July 30, 2005.

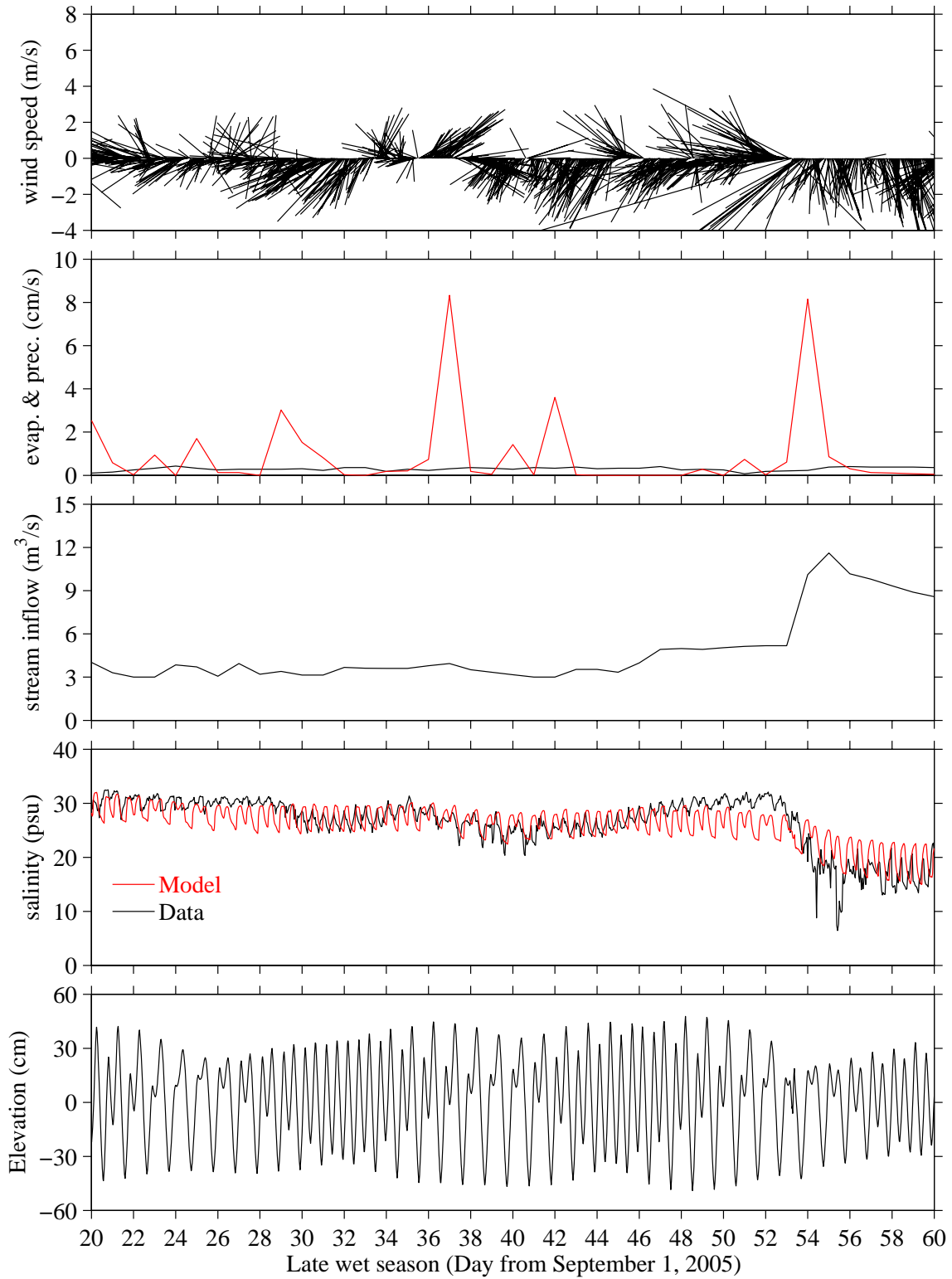


Fig. 14: Panels from up to down represent the model input of winds, precipitation (red) against evaporation (black), stream inflow at hwy 41, model output salinity (red) and observed salinity (black) at HC, and model output sea level in HC for late wet season period of September 20 through October 30, 2005.

The time series of model-predicted salinities sampled at HC, Shell Island, Hall Bay, and west RB (locations shown in Fig. 1) along with the freshwater discharge rates for three model simulations are presented Fig. 15. The model results show that the salinity simulations are remaining stable over the full 4 months of the prognostic simulations. Model-predicted salinity responds to semidiurnal tidal variation (two high and two low salinity each day), as well as to freshwater inflow variation. For instance, the freshwater discharge rate increases from 180 ft<sup>3</sup>/s on October 23 to 350 ft<sup>3</sup>/s on October 24, correspondingly the mean salinity decreases about 3 psu from 10/23 to 10/24.

When the freshwater discharge rate increases 50 ft<sup>3</sup>/s from its realistic rate, the mean salinities decrease 2.7 psu at HC, 2.0 psu at Shell Island, and 1.9 psu at Hall Bay and west RB, respectively. When the freshwater discharge rate increase 100 ft<sup>3</sup>/s from its realistic rate, the mean salinities decrease 4.9 psu at HC, 4.3 psu at Shell Island, 3.4 psu at Hall Bay, and 3.3 psu at west RB, respectively. The largest decrease occurs at HC since this location is closest to the freshwater input location. It should be noted that increasing the freshwater inflows to HC not only decreases the salinity in HC, but also significantly affects salinity over the entire RB estuary complex. Such finding demonstrates the necessity of using a model such as the one applied here in order to answer such environmental managements questions.

## 6.2. Scenario 2

In this scenario, the freshwater inflows to NB through the Golden Gate canals were decreased by 350 ft<sup>3</sup>/s from their realistic values during the early wet season (June to September). The intent was to investigate what might happen under a fresh water storage scenario. By virtue of having the extended NB portion of our model (again not included in the original proposal but anticipated as a need) we were able to accommodate this scenario experiment request. We ran two model simulations each from June 1 through July 30, 2005 using two different freshwater inflows at the upstream end of NB. The first used the realistic freshwater inflow collected from SFWMD, and the second subtracted 350 ft<sup>3</sup>/s from the realistic discharge rates.

The time series of model-predicted salinities and elevations sampled at upper NB, middle NB, and lower NB (locations shown in Fig. 1) along with the freshwater discharge rates for two model runs are presented Fig. 16. The model simulated elevation results show that the sea levels at these 3 locations are very similar for both tidal amplitudes and phases (lower panel at Fig. 16). For amplitude, it is about 5 cm higher at the upper portion of NB than at the lower portion. For phase, there is about a half hour lag at the upper portion relative to the lower portion of NB. This is because the dimension of the NB is relatively small and shallow. The model-simulated salinities for two runs show that by decreasing the fresh water inflow rates by 350 ft<sup>3</sup>/s, the mean salinity increases by about 4.0 psu at the upper (panel 2 at Fig. 16), 5.1 psu at the middle (panel 3 at Fig. 16), and 2.2 psu at the lower (panel 4 at Fig. 16) locations of NB, respectively. It is interesting to note that the maximum mean salinity difference occurred at the middle NB location, rather than at the upper NB location. This is because even with the freshwater inflow reduced by 350 ft<sup>3</sup>/s, the salinity at the upper NB is still very small (less than 5

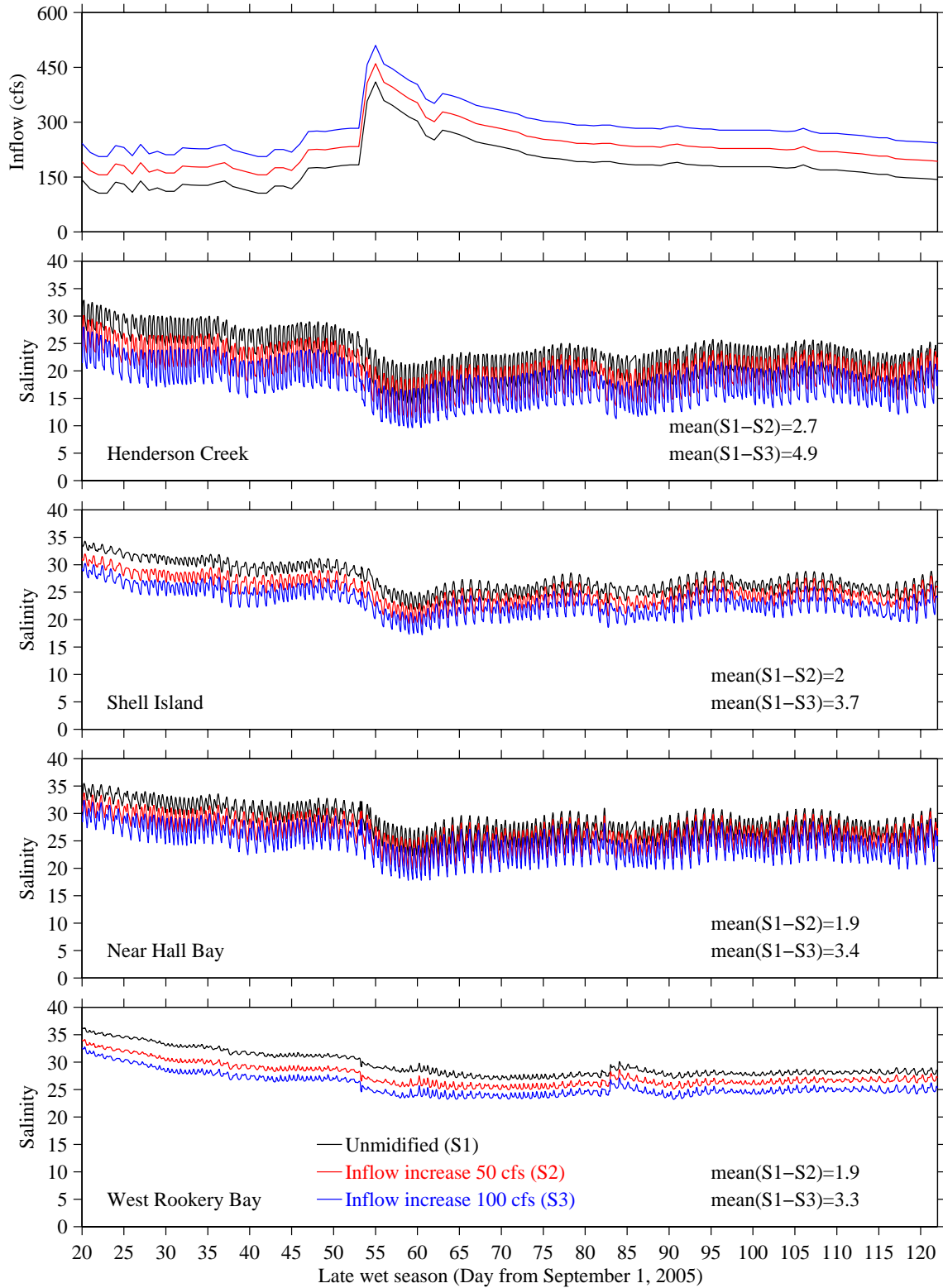


Fig. 15: Time series of model-predicted salinity sampled at HC, Shell Island, Hall Bay, and west RB (locations shown in Fig. 1) along with present freshwater inflow status (black, S1), increasing 50 ft<sup>3</sup>/s inflow (red, S2), and increasing 100 ft<sup>3</sup>/s inflow (blue, S3).

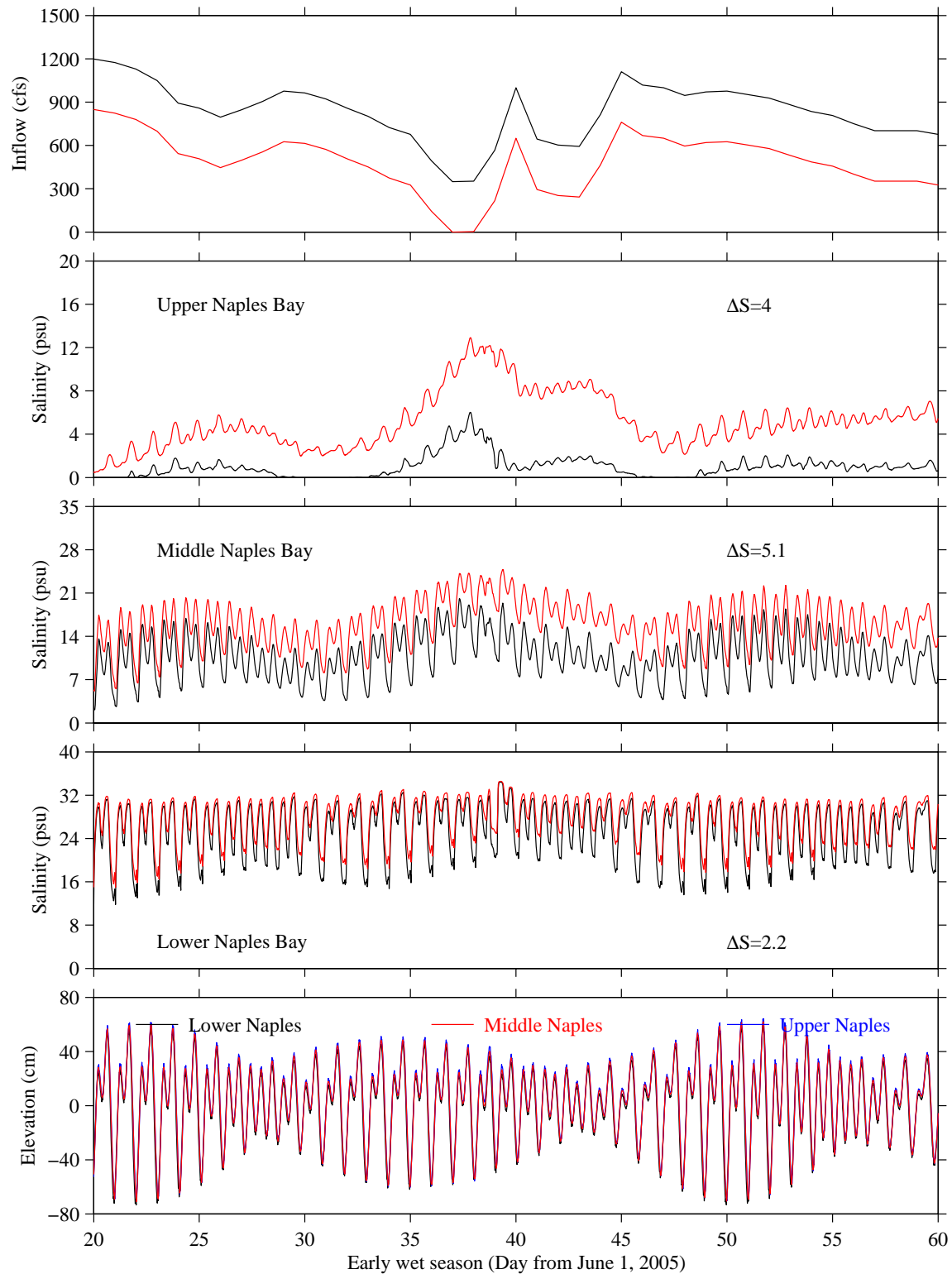


Fig. 16: Time series of model-predicted salinity and sea elevation sampled at upper NB, middle NB, and lower NB (locations shown in Fig. 1) along with present freshwater inflow status (black) and decreasing 350 ft<sup>3</sup>/s inflow (blue).

psu) during the large inflow events. Another pronounced feature is that when the freshwater inflow decreases, the salinity sampled at both the upper and middle NB varies by similar amounts through entire tidal cycle, whereas the salinity sampled at the lower NB location shows an asymmetry between periods of high and low water. This further demonstrates the need for fully 3D, baroclinic hydrodynamic models of the type provided here to ascertain the salinity behaviors of the RB and NB estuary complexes in response to regulatory modifications in fresh water inflows.

## 7. Conclusions

Proposed was the development of a hydrodynamic model to link freshwater inflow (cfs) from the Henderson Creek and Eagle Creek canals to the salinity patterns in Henderson Creek and Rookery Bay, with the understanding that the Finite Volume Coastal Ocean Model (FVCOM) of Chen et al. (2003), as applied to Tampa Bay by Weisberg and Zheng (2006), would be implemented for the Henderson Creek/Rookery Bay region and used for hindcast simulations of the combined estuary system, as driven by rivers, tides and winds and gauged against available in situ data. Based on satisfactory results we also committed to performing fresh water flow rate modification scenario experiments to investigate the salinity patterns that may result under these. This final report (together with three previous quarterly reports) provides all of the deliverables that were originally agreed to. In addition to what was originally proposed we also extended the model domain to include the Naples Bay estuary, and we performed fresh water flow rate modification scenarios for Naples Bay as well as for the Rookery Bay/Henderson Creek complex. While not reported on herein we also initiated (at no additional cost) a set of in situ measurements of currents and sea level at several locations within the Rookery Bay estuary complex to further test the veracity of the model simulations. In summary we met all of the proposal goals, and we made substantial contributions beyond those that were proposed and funded.

The 3D, baroclinic, prognostic FVCOM was applied to the combined RB and NB estuary complex (after modification of the original code to include precipitation and evaporation). Prior to attempting fully baroclinic estuary circulation simulations, we first examined the tidal circulation, drawing quantitative comparisons between the model-simulated elevations with observations at the Naples Bay NOAA-NOS tide gauge, the only sea level observations available in the model domain, to determine the model veracity with respect to tides. The results were very good, suggesting that we could use the model for describing tides over the entire model domain. Tidal currents were found to be fairly rectilinear within the RB and HC estuary system with a clockwise polarization. The tidal current amplitude was found to be generally small except at the narrow channels, where the tidal current can reach about 1.2 m/s. The total flood volume entering RB complex is about  $4.73 \times 10^6 \text{ m}^3$  during spring tides and  $2.32 \times 10^6 \text{ m}^3$  during neap tides, where about 55% flows through the inlet connecting with Johnson Bay and the other 45% flows through northwest channel.

Given the apparent success with tidal simulations we then added rivers and winds in an attempt to produce realistic baroclinic simulations of the complete estuary

circulation and to perform the scenario experiments with respect to fresh water flow rate modifications. The results for salinity when gauged against available in situ data were also good suggesting that the model is properly accounting for the 3D, baroclinic nature of the RB estuary complex circulation and salinity budget. A model simulation limitation is that we were provided only one set of river inflow data, that for the main weir #1 entering Henderson Creek. While this is the primary fresh water inlet, the lack of data from other sources may have been limiting. Moreover, while precipitation and evaporation were included in the model forcing function, the validity of these data may also be in question. Hence it is unclear whether the mismatch observed between the model simulation and the limited observations resulted from errors in the model or errors in the forcing functions. The results most likely reflect a combination of the two, although we submit that with improved model forcing functions we would expect improved results. With that being said, the results are actually quite good for both the early and late wet seasons simulated, and the inclusion of the other three freshwater inflows should provide further improvements to the model-simulated salinity. The model simulations show that by varying the freshwater inflows to HC the salinities are modified throughout the RB estuary complex.

Three sets of regulatory fresh water inflow modification scenarios were performed, two for HC and one for NB. The first two consisted of adding either 50 ft<sup>3</sup>/s or 100 ft<sup>3</sup>/s to the ambient fresh water flow rates at the main weir #1. The third consisted of diverting (reducing) the fresh water flow rate into NB by 350 ft<sup>3</sup>/s. All of these three scenarios resulted in significant salinity changes within the RB and NB estuary complexes, respectively.

As an outgrowth of this project we were able to secure a two-year graduate student fellowship for Mr. Jian Geng, now pursuing the PhD with emphasis on estuary circulation and the Rookery Bay and Naples Bay estuary complexes in particular. Mr. Geng will analyze the new data sets that are presently being collected and will draw additional comparisons with new model simulations to be conducted over the time period of the new measurements. These model/observation comparisons will further quantify the veracity of the model as developed in this completed one year grant. We intend to seek additional funding in the future consistent with our original proposal that called for a second phase of funding to complement the first phase now completed.

Some suggestions for new work and for applications of the work already completed are as follows:

- Perform additional regulatory fresh water flow rate modification scenarios as deemed necessary by the RBNERR and SFWMD.
- Set up public outreach demonstrations at the RBNERR for the purpose of illustrating how the circulation impacts the distribution of water properties throughout the RB and NB estuary complexes. In particular, provide maps of current variations for use by recreational boaters and fishers. This could be set up in a nowcast/forecast format so that the public could access this information for use in any given day.
- Other related public education demonstrations could also be developed.

- Whereas the running of the 3D, baroclinic, estuary circulation model requires computational resources that may be difficult to implement at the RBNERR itself (although output is easily ported using the internet), and hence the performance of regulatory fresh water flow rate scenarios with the full model may be problematic without external assistance, it may be possible to analyze the data to produce a simplified statistical model to the extent that the salinity variations evince relatively simple spatial patterns. While we have not pursued this yet, the initial results suggest that this is indeed the case. Through empirical orthogonal function (or principal component) analyses we anticipate being able to implement a statistical model that could be run at the RBNERR with a modest amount of computer resource and technical training.
- Being that this is the first time that a full 3D, baroclinic, estuary circulation model linked to the adjacent Gulf of Mexico has been applied to either the Rookery Bay or the Naples Bay estuary complexes there are a myriad of environmental questions that can now be addressed. We are open to discussions of such applications, and for discussions on additional data (on fresh water flow rates for model forcing and in situ data for quantifying model veracity) that would be useful to both the RBNERR and SFWMD and to the City of Naples.
- Finally, it is possible to extend the present results to:
  - other aspects of water quality
  - southward to the Ten Thousand Islands
  - the study of hurricane storm surge.

## References

- Blumberg, A. F., 1993. A Primer of ECOM-si, *Technical Report*, 73 pp., HydroQual, Inc., Mahwah, New Jersey.
- Blumberg, A. F. and G. L. Mellor, 1987. A description of a three-dimensional coastal ocean circulation model, 1-16, In: N. Heaps (ed.), *Three-Dimensional Coastal Ocean Models*, American Geophysical Union, Washington, D. C.
- Chen, C. S., H. D. Liu, and R. C. Beardsley, 2003. An unstructured, finite-volume, three-dimensional, primitive equation ocean model: application to coastal ocean and estuaries, *J. Atmospheric and Oceanic Technology*, **20**: 159-186.
- Foreman, M.G.G., 1977. Manual for tidal heights analysis and prediction, *Pac. Mar. Sci. Rep.* 77-10, Institute of Ocean Science, Patricia Bay, Sidney, B.C.
- Haidvogel, D. B., H. G. Arango, K. Hedstrom, A. Beckmann, P. Malanotte-Rizzoli, and A. F. Shchepetkin, 2000. Model Evaluation Experiments in the North Atlantic Basin: Simulations in Nonlinear Terrain-Following Coordinates, *Dynamics of Atmospheres and Oceans*, **32**: 239-281.
- He, R. and R.H. Weisberg, 2002. Tides on the west Florida shelf, *Journal of Physical Oceanography*, **32**: 3455-3473.
- Lee, T. and B. Yokel, 1973. Rookery Bay land use studies: Environmental planning strategies for the development of a mangrove shoreline. University of Miami, Florida. 51p.
- Locker, S.D. and A.K. Wright, 2003. Benthic habitat mapping for habitat suitability modeling in Rookery Bay National Estuarine Research Reserve. Final report to Florida Marine Research Institute, Florida Fish and Wildlife Conservation Commission, St. Petersburg, Florida, 84p.
- Lynch, D. R. and C. E. Naimie, 1993. The  $M_2$  tide and its residual on the outer banks of the Gulf of Maine, *Journal of Physical Oceanography*, **23**: 2222-2253.
- Rubec, P.J., M.A. Shirley, J. Lewis, P. O'Donnell, S.D. Locker, G.E. Henderson, T. Mo, and C. Westergren, 2003. Spatial modeling to determine optimal freshwater inflows into estuarine habitats in the Rookery Bay National Estuarine Research Reserve. Final report to the South Florida Water Management District, Big Cypress Basin Board, Naples, Florida, from Florida Fish and Wildlife Conservation Commission, Florida Marine Research Institute, St. Petersburg, Florida, 83p.
- Shirley, M.A., P. O'Donnell, V. McGee, and T. Jones, 2003. Multi-dimensional scaling (MDS) analyses of fish and macro-invertebrate community structure: a comparison of three south Florida estuaries with natural and altered freshwater inflows. Manuscript

presented at the Estuarine Indicators Workshop, held at the Sanibel Captiva Conservation Foundation Marine Laboratory, October 29-31, 2003.

Shirley, M.A, V. McGee, T. Jones, B. Anderson, and J. Schmid, 2004. Relative abundance of stenohaline and euryhaline oyster reef crab populations as a tool for managing freshwater inflow to estuaries, *Journal of Coastal Research*.

Weisberg, R.H. and L.Y. Zheng, 2006. Circulation of Tampa Bay driven by buoyancy, tides, and winds, as simulated using a finite volume coastal ocean model. *Journal of Geophysical Research*, **111**, C01005, doi:10.1029/2005JC003067.